HAL
open science

Rovibrational laser jet-cooled spectroscopy of SF 6 –rare gas complexes in the ν 3 region of SF 6

Pierre Asselin, Andrew C Turner, Laurent Bruel, Valérie Brenner, Marc-André Gaveau, Michel Mons

To cite this version:

Pierre Asselin, Andrew C Turner, Laurent Bruel, Valérie Brenner, Marc-André Gaveau, et al.. Rovibrational laser jet-cooled spectroscopy of SF 6 –rare gas complexes in the ν 3 region of SF 6. Physical Chemistry Chemical Physics, 2018, 20 (44), pp.28105-28113. 10.1039/c8cp04387f . hal-02344506

HAL Id: hal-02344506

https://hal.science/hal-02344506

Submitted on 4 Nov 2019

HAL is a multi-disciplinary open access archive for the deposit and dissemination of scientific research documents, whether they are published or not. The documents may come from teaching and research institutions in France or abroad, or from public or private research centers.

L'archive ouverte pluridisciplinaire **HAL**, est destinée au dépôt et à la diffusion de documents scientifiques de niveau recherche, publiés ou non, émanant des établissements d'enseignement et de recherche français ou étrangers, des laboratoires publics ou privés.

Rovibrational laser jet-cooled spectroscopy of SF_6-rare gas complexes in the ν_3 region of SF_6

Pierre Asselin[a], Andrew C. Turner[b], Laurent Bruel[c], Valérie Brenner[d], Marc-André Gaveau[d] and Michel Mons[d]

[a]*Sorbonne Université, CNRS, MONARIS, UMR 8233, 4 place Jussieu, Paris, F-75005 France.*
[b]*Department of Earth and Planetary Science, University of California, Berkeley, California 94720 USA.*
[c]*CEA Marcoule, DEN, 30207 Bagnols-sur-Cèze, France*
[d]*LIDYL, CEA, CNRS, Université Paris-Saclay, CEA Saclay 91191 Gif-sur-Yvette France*

Abstract

High resolution infrared spectroscopy combining an external cavity quantum cascade laser with a pulsed pin hole supersonic jet is used to investigate small van der Waals (vdW) hetero clusters containing SF_6 and rare gas (Rg) atoms in the ν_3 region of SF_6. In a first analysis, the rovibrational band contours of parallel and perpendicular transitions of 1:1 SF_6-Rg hetero dimers (Rg = Ar, Kr, Xe) are simulated to derive ground and excited state parameters and hence ground state and equilibrium S-Rg distances with a precision better than 0. 5 pm. These values are used to assess quantum chemistry calculations (DFT-D method) as well as semi-empirical predictions (combination rules). In a second step, the spectral signatures of the 1:1 heterodimers and of larger heteroclusters containing up to three Rg atoms have been identified by considering reduced vibrational red shifts, i.e., shifts normalized to the average 1:1 red shift. The reduced vibrational red shifts within the series of bands observed and assigned to 1:1 and 1:2 complexes are found to be independent upon the Rg atom, which suggests similar 1:1 and 1:2 structures along the Rg series. In addition, the increasing number of bands when going from monomer to 1:2 complexes illustrates the increased lifting of vibrational degeneracy induced by Rg solvation. Finally, the vibrational shifts of the 1:1 SF_6-Rg hetero dimers are found to fit an intermolecular interaction model in which long–range attractive and short-range repulsive contributions to the vibrational shift are found to partially compensate, the former being dominant. From the same model, well depths are obtained and are found to compare well with quantum chemistry calculations and semi-empirical combination rules.

I- Introduction

Weak intermolecular forces such as van der Waals interactions play an important role in molecular sciences, ranging from the control of the conformational landscape of flexible biomolecules to the structure of molecular crystals.[1] These non-covalent interactions are much weaker than covalent bonds and even hydrogen bonds but their multicentric character leads to a significant contribution which turns out to control the structures and properties of van der Waals (vdW) molecular complexes. High resolution spectroscopy has proved to be a suitable method to provide information on the structures and intermolecular interactions of these systems: in the microwave region a large number of studies using molecular beam electric resonance[2] or pulsed nozzle Fourier transform techniques[3] enabled the characterization of

structure and internal dynamics in the ground state. In the near-UV region, laser induced fluorescence electronic spectroscopy has been used to provide a detailed description of the solvation of aromatic molecules by rare gas atoms and document the role of vdW modes in molecular dynamics.[4,5]

The development of high resolution (HR) infrared (IR) spectroscopy in supersonic jets has allowed direct determinations of the potential energy surface (PES) of several diatomic (HF, HCl)[6,7,8,9] and linear triatomic molecules such as CO_2,[10,11,12] N_2O[13,14] and OCS[15,16,17] interacting with rare gases (Rg). For more details the reader can refer to the website devoted to the bibliography of weakly bound complexes (involving Rg or not).[18] The rovibrational analysis of such small complexes provided very precise structural parameters used to model the intermolecular PES. The dynamical picture is indeed more challenging in the case of floppy weakly bonded vdW Rg complexes with partners having large amplitude motions such as H_2O[19,20] and NH_3[21,22]: HR IR spectra of such complexes directly probe the rovibrational states related to a nearly flat PES with low energetic barriers along angular coordinates of the species. Compared to microwave spectroscopy, very few infrared studies have been reported so far about mixed vdW clusters associating rare gases and large polyatomic molecules.[18,23,24,25,26] Taking advantage of powerful line-tunable cw CO_2 lasers, Gough et al.[24] implemented infrared photofragmentation spectroscopy in molecular beams to study the low resolution IR spectrum of argon clusters seeded with a single SF_6 molecule in the spectral region of the triply degenerate ν_3 vibration at 948 cm^{-1}. The ν_3 band of SF_6 in SF_6 clusters was found to shift monotonically to the red when increasing the backing pressure as a consequence of increasing average cluster size. Thereafter, Hartmann et al.[27] achieved the first high resolution laser spectroscopic study of vdW clusters of SF_6 and mixed SF_6-rare gas clusters in helium droplets at 0.37 K. Partially resolved rotational contours split into parallel and perpendicular bands are observed but no structural information transposable to the gas phase could be extracted.

In a recent paper, we reported a high resolution infrared laser jet-cooled study of the SF_6 dimer and $(SF_6)_2$-Rg heterotrimers in the ν_3 mode region.[28] Taking advantage of our versatile set-up, various experimental conditions of nozzle geometry, axial distance and SF_6 concentration were explored to revisit the conformational landscape of the SF_6 dimer.

The present paper is devoted to the spectroscopic characterization of the 1:1 SF_6-Rg heterodimers in the ν_3 mode region using the same infrared tunable laser spectrometer recently implemented in our laboratory. The high resolution rovibrational spectra of parallel and perpendicular bands of SF_6-Rg complexes enable us to extract precise S-Rg bond lengths and band origin shifts. Lastly, vibrational signatures assigned to larger heteroclusters up to SF_6-$(Rg)_3$ on the red side of the 1:1 heterodimer constitute an interesting benchmark to test the evolution of red shift with cluster size at least for the first solvation steps. These experimental data are then used to parameterize a simple model for the intermolecular potential.

II- Experimental details

The vibration-rotation spectra of SF_6-rare gas clusters have been recorded using an external-cavity quantum cascade laser (EC-QCL) coupled to a pulsed supersonic jet. This set-up has been already described in previous papers[28,29] and only the main characteristics will be described in the present study.

The light source is a continuous-wave room-temperature mode-hop-free EC-QCL with a spectral width of 10 MHz, which covers the 930-990 cm^{-1} range (Daylight Solutions). About 8% of the total light power (about 120 mW around 950 cm^{-1}) is sent through two laser channels for relative and absolute frequency calibrations. The remaining light is sent through a multipass astigmatic cavity according to a 182-pass pattern which crosses almost perpendicularly the jet expansion.

In our recent study on pure $(SF_6)_2$ and mixed $(SF_6)_2$-rare gas clusters,[28] molecular complexes were stabilized regardless of the geometry of the supersonic expansion used, which enabled to vary the rotational temperature (between 3 K and 0.8 K, respectively in planar and axisymmetric expansions under comparable generating conditions) and promote one conformer with respect to the other. In the present work, (SF_6)-Rg complexes were investigated in the same manner from the expansion of a molecular jet at very high dilution of a SF_6/Rg mixture (corresponding to about 1% of the total gas flow injected for Ar, Kr and Xe) seeded in helium at backing pressures as high as 8 bar. Two nozzle geometries were tested: a pulsed circular pin hole nozzle (General Valve Series 9) in standard configuration with a 0.35 mm diameter (D) pin hole and a slit nozzle obtained by fitting the pin hole nozzle with two modified industrial blades, forming a 30 mm length x 50 µm width (l) slit opening. With the pin hole nozzle, the van der Waals heterodimers were formed and rotationally cooled at temperatures T_R below 1 K and then probed by the many infrared laser spots distributed in a broad region of the expansion, at *z* average distances from the nozzle comprised between 9 and 18 mm with a length Δz of about 10 mm. These *z* values correspond to a range of reduced distances *z*/D between 25 and 50. A good balance between efficient rovibrational cooling and high molecular density was found at about *z* = 15 mm (z/D = 43) for the present pin hole jet expansions with translational temperatures largely below 1 K in the region Δz probed.

Our rapid scan scheme is similar to previous designs developed for high resolution molecular spectroscopy.[30] A baseline-free transmittance through the multipass cavity is obtained by taking the ratio of signals recorded in presence and absence of the jet (by opening or not the valve). The procedure for absolute frequency calibration is achieved *a posteriori* by measuring the deviation between experimental and HITRAN12 database C_2H_4 frequencies to correct the free spectral range value of the etalon fixed at the beginning of each experiment. The accuracy of the frequency calibration is around 0.0005 cm^{-1}.

III Experimental results

Guided by the results of previous infrared experiments on SF_6-Rg clusters,[24,27] rovibrational signatures have been searched on the red side of the ν_3 band origin of SF_6 monomer using SF_6/Rg equimolar mixtures and different dilutions of SF_6 in He at backing pressures of 8 bar. While SF_6-Rg clusters are expected to be more easily detected in planar expansions due to a weaker Doppler broadening compared to pin hole jets[28,31] no SF_6-Rg

complex absorption could be detected with the slit nozzle at any dilution used. The absence of such 1:1 complex signals can be ascribed to a lower stability of the 1:1 complex compared to the homodimer, which hampers their observation in the higher temperature conditions of planar expansions. On the other hand, new bands were observed on the red side of the SF_6 monomer ν_3 band and assigned to SF_6-Rg (Rg = Ne, Ar, Kr, Xe) 1:1 clusters when replacing with the pin hole nozzle. The 1:1 absorption signal observed was maximized by tuning the SF_6:Rg ratio to 1:8 for heavier rare gases and 1:100 for Ne. Due to the very close presence of the intense ν_3 band of SF_6 monomer, jet-cooled spectra of SF_6 monomer were recorded with the same SF_6/He dilution as that used with the SF_6/Rg/He ternary mixtures, and then subtracted to isolate the contribution of the vdW SF_6-Rg heterodimers. Figure S1 (in the SupMat file) displays the example of the SF_6-Ar spectrum, exhibiting a large contribution of the SF_6 monomer ν_3 band which can be efficiently removed following this subtraction procedure. Figure 1 displays the four EC-QCL jet-cooled spectra of SF_6-Rg for Rg = Ne, Ar, Kr and Xe after subtraction.

Rotational analyses

By analogy with the the SF_6 dimer,[28] it is expected to observe parallel and perpendicular bands of SF_6-Rg arising from the degeneracy lifting of the triply degenerate state (ν_3) of the SF_6 monomer in complexes of C_{3v} symmetry, in which the Rg atom lies above the center of a face of the SF_6 octahedral molecule.

Q-branch maxima of parallel bands for SF_6-Ar, SF_6-Kr and SF_6-Xe are clearly visible (Fig. 1) at 946.977, 946.638 and 946.221 cm^{-1}, respectively with well resolved *P*- and *R*-branch structures. The *K* structure is not resolved within our experimental linewidth (150 MHz), limited by residual collisional and Doppler broadenings. For the three heaviest rare gases, *Q*-branch maxima of SF_6-Rg bands exhibit increasing red shifts with respect to the ν_3 band of SF_6, reaching values up to 1.8 cm^{-1} for SF_6-Xe. With Ne, the red shift is so weak that several features of the SF_6-Ne spectrum overlap with intense *P* branch lines of the SF_6 monomer band, which prevented any rovibrational analysis. A sharp maximum is observed at about 947.86 cm^{-1} but no splitting between parallel and perpendicular bands could be evidenced in agreement with the helium droplet study[27].

All perpendicular bands display characteristic ${}^{P,R}Q(J,K)$ branches, in particular very strong ${}^{R}Q(J,0)$ ones at 947.392, 947.175 and 946.897 cm^{-1} for SF_6-Ar, SF_6-Kr and SF_6-Xe, respectively, as well as broader ${}^{P}Q(J,K>0)$ and ${}^{R}Q(J,K>0)$ branches, observed on both sides of ${}^{R}Q(J,0)$. Similarly to the perpendicular band of the SF_6 dimer, SF_6-Kr and SF_6-Xe complexes display a first-order Coriolis interaction, as proven by experimental spacings between nearby *Q* branch peaks, which are close to the calculated value of $2(A(1-\xi)-B)\approx$ 0.027 cm^{-1} for SF_6-Kr and 0.034 cm^{-1} for SF_6-Xe, by taking the Coriolis parameter ξ equal to that of the SF_6 monomer, 0.69374.[32]

From the perpendicular band contour of SF_6-Ar, the first-order Coriolis interaction is more difficult to identify: very few intense ${}^{R}Q(J,K>0)$ branch peaks at 947.409, 947.422 and 947.435 cm^{-1} are found to be spaced by 0.013 cm^{-1} in agreement with the calculated spacing value while ${}^{P}Q(J,K>0)$ branch peaks are too weak to be observed. Additionally, a series of

intense features is observed on the R branch side with a spacing ranging between 0.055 and 0.063 cm^{-1}, which could belong to $^{R}R(J,K)$ or $^{P}R(J,K)$ lines.

Our experiments confirm the reduction of the three-fold degeneracy of the ν_3 mode of the SF_6 monomer through a first-order Coriolis interaction, consistent with the existence of *A* and *E* states in complexes of C_{3v} symmetry. A two-step band contour analysis was carried out: firstly, the three parallel bands of SF_6-Ar, SF_6-Kr and SF_6-Xe (Figure 2) were simulated according a symmetric top structure in order to derive best fit molecular parameters $\nu_{//}$, *A'*, *B''* and *B'*. The ground and ν_3 excited states experimental rotational constants were used to obtain accurate experimental ground state (R_0) and equilibrium (R_e) distances of SF_6-Rg complexes, (Table 1), assuming an unchanged monomer structure upon heterodimer formation. Secondly, perpendicular bands were simulated by fixing *A''* to the *ab initio* value and *B''* to the value derived from the parallel band contour simulation to obtain the best fit molecular parameters *A'*, *B'*, $\nu_{\perp}$ and ξ. Figure 3 displays the satisfactory comparison between jet-cooled perpendicular band spectra of SF_6-Kr and SF_6-Xe and our best simulations. In contrast, the observed perpendicular band of SF_6-Ar could not be correctly fitted : the small number of $^{R}Q(J,K>0)$ branch bands prevented us to carry out a rovibrational analysis. Table 1 reports the sets of molecular parameters derived from these band contour analyses. The transition frequencies of parallel and perpendicular bands of the SF_6-Rg heterodimers are listed in the Table S1 of Supplementary Material File. Finally one can notice that, in contrast to our previous work on SF_6 dimers[28], no spectroscopic evidence for the presence of ternary SF_6-Rg-He clusters could be found, presumably because of a too weak binding energy of the helium atom to the heterodimers under the present jet conditions.

Spectral shifts

On the red side of both parallel and perpendicular bands of heterodimers, ten additional weaker bands are observed: at 946.693, 946.483, 946.220 and 945.664 cm^{-1} in the SF_6-Ar spectrum, at 946.241, 945.938, 945.612 and 945.320 cm^{-1} in the SF_6-Kr spectrum and at 945.857 and 945.371 cm^{-1} in the SF_6-Xe spectrum (indicated by stars in Figure 1). The corresponding red shifts range between 1 and 3 cm^{-1}, which is consistent with the signature of larger heteroclusters containing up to three Rg atoms, assuming a red shift additivity rule. In addition, since the larger complexes are expected to exhibit a complete degeneracy lifting of the ν_3 vibration, a set of three bands can be anticipated for each of them, leading to increased complexity of the spectral pattern. In order to assign the spectra and assess their robustness relative to the nature of the rare gas, reduced red shifts have been considered (Table 2), i.e., red shifts normalized to the average red shift $\Delta\nu_{1:1}$ measured for the corresponding 1:1 complex, which is defined as :

$$\Delta\nu_{1:1} = (\Delta\nu_{//} + 2\Delta\nu_{\perp})/3 \qquad (1)$$

where $\Delta\nu_{//}$ and $\Delta\nu_{\perp}$ correspond to the red shift of parallel and perpendicular bands, respectively.

For the 1:1 complexes, reduced red shifts obtained for both the parallel and perpendicular bands are nearly independent upon the nature of the rare gas, with values close to 0.81 and 1.36 respectively. This suggests comparable structures and symmetry for this

complex along the rare gas series, in agreement with the C_{3v} symmetry anticipated, due to three simultaneous F-Rg close contacts. Interestingly, the three next reduced shifts obtained along the series of Ar, Kr and Xe rare gases beyond the 1:1 complex also turn out to be nearly independent upon the nature of the rare gas, with values close to 1.7, 2.0 and 2.4, and an average value of about 2.0.

IV Discussion

Comparison between experimental and theoretical structural parameters

The ground and excited state rotational constants derived from the present study provide reliable intermolecular and R_e distances for the three SF_6-Rg complexes containing heavier rare gases (Table 1) with an accuracy ranging between 0.13 pm for SF_6-Xe and 0.44 pm for SF_6-Ar. It is worth comparing experimental R_e distances with both *ab initio* calculations and simple theoretical models to evaluate the predictive character of these methods.

In order to account for the dispersive character of the vdW SF_6-Rg interactions, geometry optimizations have been carried out using density functional theory corrected by explicit dispersion terms (DFT-D), at the RI-B97-D/def2-TZVPPD level of theory with the D3 type Grimme correction (including the Becke-Johnson damping and three-body terms), and using an adapted pseudo potential (effective core potential) for Xe.[33] All calculations were carried out using the TurboMole[34] package. This method was first validated on purely dispersive Rg-Rg dimers, as a test case before applying it to SF_6-Rg systems. Relative discrepancies ranging between 3 and 7 % were obtained for these homodimers , always with an overestimation of the Rg-Rg distances, compared to distances derived from various fitting procedures of experimental data. [35,36,37,38] Geometry optimization of the SF_6-Rg complexes were carried out, either with or without a C_{3v} geometry constraint. The C_{3v} geometry minima are found to be saddle points connecting three minima of C_s symmetry. For the three heavier Rg atoms from Ar, the (three equivalent) minima differ from the corresponding C_{3v} symmetry structure by a slight off-C_{3v} axis position of the rare gas (by less than 5 pm towards the gap between two neighbouring F atoms) and slightly shorter S-Rg distances (typically 2-5 pm). The energy difference between the C_s minima and the C_{3v} saddle point is lower than 0.3 kJ/mol (i.e. 13 % of the SF_6-Ar well depth, and 7 % for the heavier rare gases). Such a peculiarity suggests a relatively flat surface with multiple minima for the motions of the Rg perpendicularly to the C_{3v} axis, potentially already connected in the vibrational ground state, since the intermolecular ZPE typically amounts to 0.5 kJ/mol in all three species. These results can thus be considered as compatible with the spectroscopic evidence for the C_{3v} symmetry (at least from Ar), taking vibrational averaging into account. The case of Ne is similar but differs quantitatively by an off-axis position of the Ne atom in the minimum more shifted (by 60 pm) than with heavy rare gases. The energy difference between the off-axis C_s minima and the C_{3v} minimum remains modest (0.26 kJ/mol) but the relative variation is larger than with heavier atoms (~21%) due to a smaller well depth ; from the similar intermolecular ZPE than previously, the same extensive vibrational averaging can be expected. The R_e distances obtained from DFT-D calculations (Table 3) compare well with the experimental

data, with a relative discrepancy in the 2-3% range weaker than in the Rg-Rg dimers (see above), neglecting any averaging effect due to zero point vibrational energy.

The same $R_e(SF_6–Rg)$ distances can be also predicted from the combination rules (CR),[39,40] currently used to derive the vdW Lennard-Jones well depths and equilibrium interatomic distances from $R_e(SF_6–SF_6)$ of $(SF_6)_2$ and $R_e(Rg–Rg)$ of $(Rg)_2$ homodimers. For our comparisons, the distance of heterodimers is obtained from the arithmetic mean of the vdW radii of corresponding homodimers, i.e. $R_e(SF_6–Rg) = \frac{1}{2}[R_e(SF_6–SF_6) + R_e(Rg–Rg)]$. The $R_e(SF_6–SF_6)$ value of 470.5 pm has been taken from Aziz et al.[41] who derived it from virial data, viscosity and a Morse-Morse-Spline-van der Waals (MMSV) potential; for the $R_e(Rg–Rg)$ distances, values experimentally determined from the fit of literature data have been used.[35-38] The $R_e(SF_6–Rg)$ distances predicted from the combination rules[40] (Table 3) are in good agreement with the present R_e measurements, with a -1.2(5) % deviation in average with respect to experiment, suggesting that the combination rules provide a relevant alternative to quantum chemistry calculations, at least at the level of theory used. Owing to the opposite trends of these theoretical approaches (systematic overestimation vs. underestimation of the R_e distances from DFT-D calculations and combination rules, respectively), the theoretical results can be used to bracket the $R_e(SF_6–Ne)$ distance, which could not be deduced from the rovibrational analysis. This distance can be reasonably estimated around 405 pm, with a precision not better than 15 pm.

In the following, we will exploit these intermolecular distances as well as the parallel and perpendicular experimental shifts derived from the present high resolution jet-cooled infrared study to assess the quality of a model intermolecular potential for SF_6-Rg.

Signature of larger SF_6-$Rg_{2,3}$ heteroclusters

The red shift patterns reported in Table 2 suggest three remarks: (i) the *reduced* shift patterns observed do not depend significantly upon the rare gas considered . This result suggests that the complexes retain the same symmetry and similar geometries all along the rare gas series.. The pattern observed (number of bands and positions) are consistent with a 1:1 complex of C_{3v} symmetry and a 1:2 complex of lower symmetry, with partially and fully lifted ν_3 degeneracy. (ii) a red shift additivity rule seems to hold, if one considers the average reduced red shift of the bands assigned to the 1:2 complex. (iii) beyond the SF_6-Rg_2 signatures, the two remaining bands are assigned to SF_6-Ar_3 and SF_6-Kr_3 heterotetramers. Their reduced shifts are around 3, as expected from the additivity rule, but are either above or below 3, which suggests that these bands do not correspond to the same vibrational component.

These measurements are remarkably consistent with an addition of vibrational shifts when increasing the number of Rg atoms. Moreover, the present frequency shift increment of 0.72 cm^{-1} per argon atom agrees well with that roughly derived from photofragmentation experiments[23] which measured a total shift of 7 cm^{-1} for SF_6-Ar_n clusters distributed between n = 1 and 12, leading to an average shift of 0.6 cm^{-1} per argon atom.

Vibrational shift and intermolecular potential for SF_6-Rg

Theoretical models were developed in the past to predict the vibrational frequency shifts of complexes between molecules of high symmetry (SiF_4, SF_6) and rare gases.[25,42,43]. One of the issues, in particular, was to determine the several physical contributions to the shifts observed.

For such systems, a first attempt to model the band shift in the SF_6-Ar_n clusters assumed that it is controlled by a dipole-induced dipole mechanism, where the vibrationally-induced instantaneous dipole of the SF_6 molecule interacts with the dipole induced in the Rg atom environment.[42] Though the model provided red shifts, it proved to be unable to reproduce the relative shifts of the parallel and perpendicular bands, even despite taking into account additional atom-atom pairwise contacts.

An alternative approach consists in considering directly the effects of vibrational excitation of the SF_6 molecule on the parameters that describe the intermolecular potential. Such an approach was developed by Howard and coworkers, in their study of linear molecules (N_2O, CO_2 and OCS) in interaction with rare gases[,11,1316]. Following their approach, we describe the interaction between the highly symmetric SF_6 molecule with a rare gas atom by a radial one-dimensional Buckingham-type potential of the form[44]

$$V(R) = Ae^{-\beta R} - C_6/R^6 \qquad (2)$$

and assume that the spectral shift effects are described by changes in the repulsive A and β, and attractive C_6 parameters upon vibrational excitation of the SF_6 molecule.
In this model, the intermolecular distance at the minimum R_e obeys the following relationship

$$\beta A e^{-\beta R_e} = 6C_6/R_e^7 \qquad (3)$$

and the well depth ε at the minimum (ε>0) is given by

$$\mathcal{E} = \frac{C_6}{R_e^6}/(1 - 6/\beta R_e) \qquad (4)$$

Vibrational excitation induces a change of the repulsive and attractive parameters, ΔA and ΔC_6 respectively, while the change in repulsive parameter β is assumed to be negligible. Under these assumptions, the change in the position of the radial minimum is obtained by differentiating Eqs (3) and (4) and can be expressed in the form

$$\Delta R_e = (\frac{\Delta A}{A} - \frac{\Delta C_6}{C_6})/(\beta - 7/R_e) \qquad (5)$$

The resulting change in the well depth is given by

$$(\Delta\mathcal{E}/\mathcal{E}) = \left(\frac{\beta R_e}{\beta R_e - 6}\right)[\frac{\Delta C_6}{C_6} - \left(\frac{\Delta A}{A}\right)\frac{6}{\beta R_e}] \qquad (6)$$

Considering that the relative variations of ZPE due to intramolecular SF_6 vibrations remain negligible, $\Delta\mathcal{E}$ can be replaced by $-\Delta\nu_{exp}$. From Eq.(6), it appears that the fractional change in the well depth results from a delicate balance between the change in attractive and repulsive contributions.

An important question is to determine how these terms vary along the series of the SF_6-Rg complexes observed. On a one hand, the long range attractive forces scale with the polarizability α of the Rg atom which defines the usual order of well depths from Ne to Xe. On vibrational excitation of SF_6, only the properties of SF_6 do change and it is therefore expected that the fractional change in attraction $\Delta C_6/C_6$ should be independent upon the nature of the Rg atom. On the other hand, the repulsive forces between the Rg atom and each of the atoms of SF_6 are modulated by the individual motions of the atoms in SF_6. The change in the repulsion term $\frac{\Delta A}{A}$ can be approximated to $(\beta^2/2)\Delta x^2$ where Δx^2 represents the change in the square of the amplitude of vibrational motion and should be identical for all the complexes of the same series. Hence $\frac{\Delta A}{A}$ at given R_m only depends on β^2, and Eq.(6) becomes:

$$\Delta\nu_{exp}\ (R_e^6/C_6) = (3\beta/R_e)\Delta x^2 - \Delta C_6/C_6 \qquad (7)$$

Owing to the independence of the Δx^2 and $\Delta C_6/C_6$ upon the rare gas, a linear dependence should be observed between the terms $\Delta\nu_{exp}\ (R_e^6/C_6)$ and $(3\beta/R_e)$, according to Eq. (7). In order to check this, the relevant parameters have been quantified: R_m are taken from the present experimental data or from combination rules (case of Ne, see Table 3) ; the repulsion parameters β and the vdW coefficients C_6 for all SF_6-Rg heterodimers have been derived according to a procedure detailed in the Supplementary Material).

Table S4 in the Supplementary Material gathers all the parameters required to plot the graph of $\Delta\nu_{exp}\ (R_e^6/C_6)$ as a function of $(3\beta/R_e)$ (see Fig. 4). Satisfactorily, a linear dependence is observed with a standard deviation of 2 x10^{-4}, providing a slope Δx^2 of 0.00421(53) $Å^{-2}$ and an intercept $-\Delta C_6/C_6$ equal to - 0.0167(14). The strong uncertainties about the R_e distance and the vibrational shift of the SF_6-Ne heterodimer explain why a significant deviation with respect to the linear dependence is observed with Ne (Fig. 4). However the accurate parameters derived from spectra with heavier rare gases clearly validate the modelling approach which accounts for the interaction whatever the rare gas partner. From these data, the contributions of the attraction and repulsion terms to the shift relative to the well depth can be estimated from Eq. 7, derived from Eq. 6.

$$(\Delta\nu_{exp}/\mathcal{E}) = \left(\frac{\beta R_e}{\beta R_e - 6}\right)\left[\frac{3\beta}{R_e}\Delta x^2 - \frac{\Delta C_6}{C_6}\right] \qquad (8)$$

The term $\left(\frac{\beta R_e}{\beta R_e - 6}\right)$ being nearly independent from the rare gas (~1.53), one obtains a negative relative shift (red shift) due to the attractive contribution of ~ -2.5 %, independently of the Rg atom. The dependence of the shift upon the rare gas essentially arises from the repulsive term, through $3\beta/R_e$, whose blue shift relative contribution amounts to +2.1% with Ne and decreases to +1.6 % with Xe. As a matter of fact, these contributions of opposite signs

nearly compensate each other, especially in the case of Ne, rationalizing the dependence of the shift upon the rare gas.

Interestingly enough, the validity of the model along the Rg series provided by the linear correlation of Fig. 4 suggests to use the corresponding parameters to derive the well depth Ɛ of these complexes (Table 4). These values are compared (Table 4) to the results of simple combination rules from well depths of Rg and SF_6 homodimers,[41,45] as well as to the BSSE-corrected RI-B97-D3/def2-TZVPPD interaction energies obtained in the present work. The agreement between these three sets of data is remarkable; the DFT-D values lying between the two sets of well depths obtained from the application of combination rules and the fit of the Buckingham model As expected the well depth ε increases dramatically from Ne to Xe, typically by a factor 3. This trend is still more marked when dissociation energies D_0 are considered (Table 4).

Conclusion

The present work reports an high-resolution IR spectroscopic study of the 1:1 SF_6-Rg (Rg = Ne, Ar, Kr, Xe) heterodimers in the region of the ν_3 band of SF_6 monomer, carried out using the infrared tunable quantum cascade laser spectrometer coupled to a pulsed supersonic jet developed in Monaris.[28] Accurate ground state and equilibrium S-Rg distances for Rg = Ar, Kr , Xe are derived from the rovibrational analysis of parallel band contours of the ν_3 transition, which are used to assess DFT-D quantum chemistry calculations and semi-empirical approaches (combination rules). For these 1:1 complexes, the similarities in vibrational shift pattern for the parallel and perpendicular bands along the Rg series, together with the rotational analyses, suggest similar C_{3v} symmetry structures all along the series. The vibrational red shifts observed along the 1:1 SF_6-Rg heterodimer series are found to be consistent with a one-dimensional radial Buckingham PES, whose analysis suggests that the shift is controlled by a subtle equilibrium between attractive and repulsive contributions, which nearly compensate each other in the case of Ne. The well depths estimated from the Buckingham model compare well with semi-empirical combination rules data and with the present DFT-D calculations. Finally, the signatures of larger heteroclusters containing up to three Rg atoms are observed and rationalized assuming a shift additivity rule as well as a cluster geometry independent upon the rare gas at least for the 1:2 complex.

Funding

This work was supported by the MICHEM Labex at Sorbonne Université.

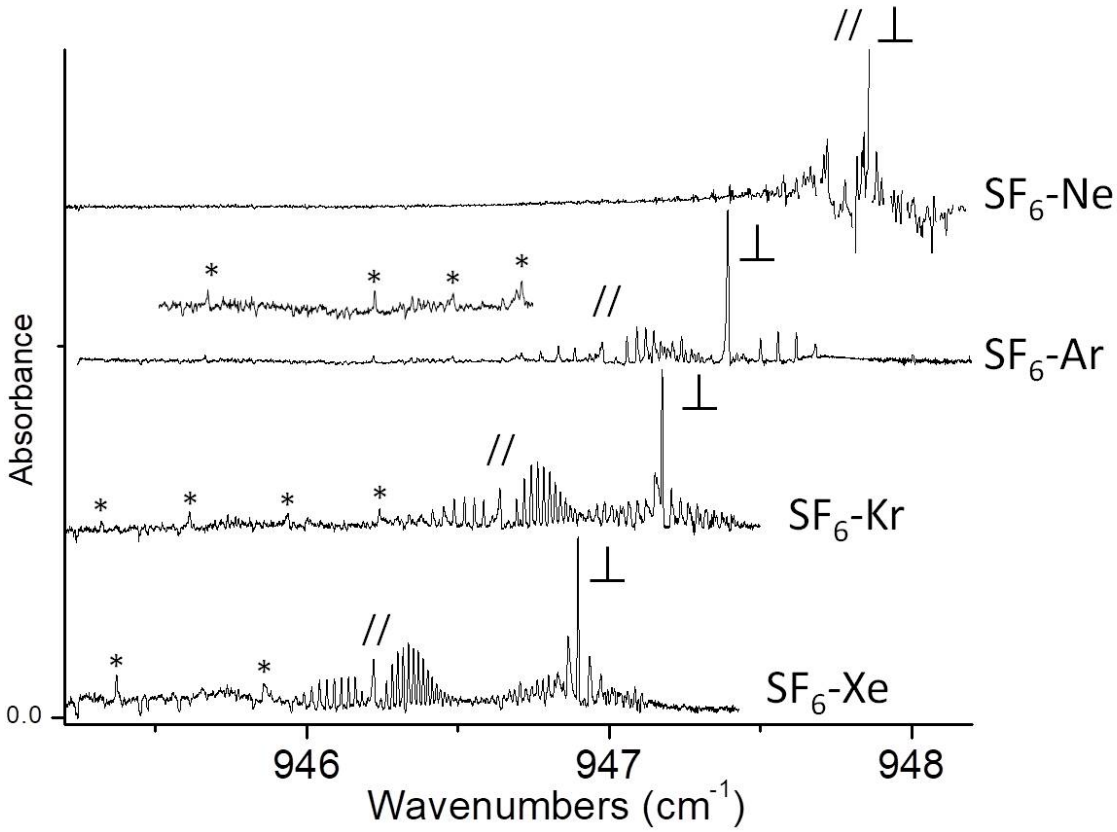

Fig.1 EC-QCL jet cooled spectra of SF_6/Rg/He mixtures diluted in 8 bar helium at an axial distance z = 15 mm for the pin hole nozzle, after subtraction of the spectrum of SF_6 monomer recorded in the same conditions of dilution of the SF_6/He mixture. The SF_6/Rg/He mixtures used are 0.12/1/100 for SF_6-Rg with Rg = Ar, Kr, Xe and 0.18/18/100 for SF_6-Ne. The // and ⊥ symbols correspond to parallel and perpendicular band contours of the 1:1 SF_6-Rg heterodimers, respectively. The bands marked by stars have been assigned to larger SF_6-$(Rg)_{2\text{-}3}$ heteroclusters.

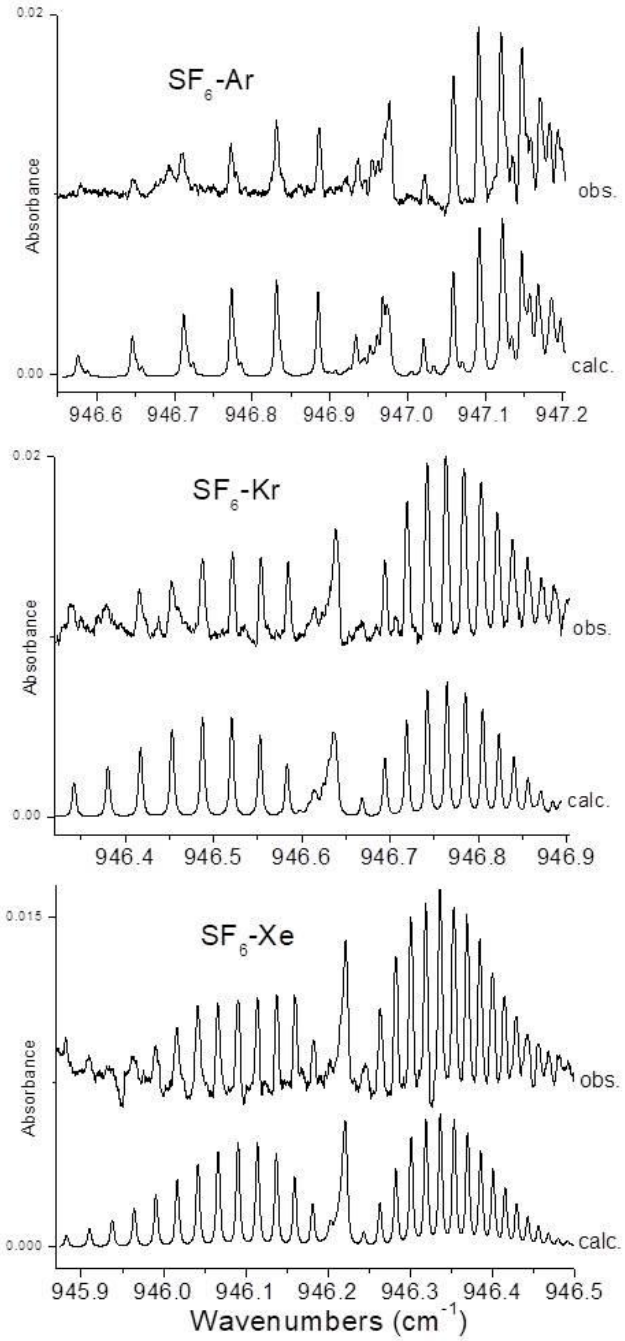

Fig. 2: EC-QCL jet cooled pin hole spectra of both ν_3 parallel bands of SF_6-Rg heterodimers (Rg=Ar, Kr, Xe) with 0.12 % SF_6 and 1% Rg diluted in 8 bar helium at an axial distance z = 15 mm, compared to our best simulation. The rotational temperature used for these simulations is 0.7(1) K.

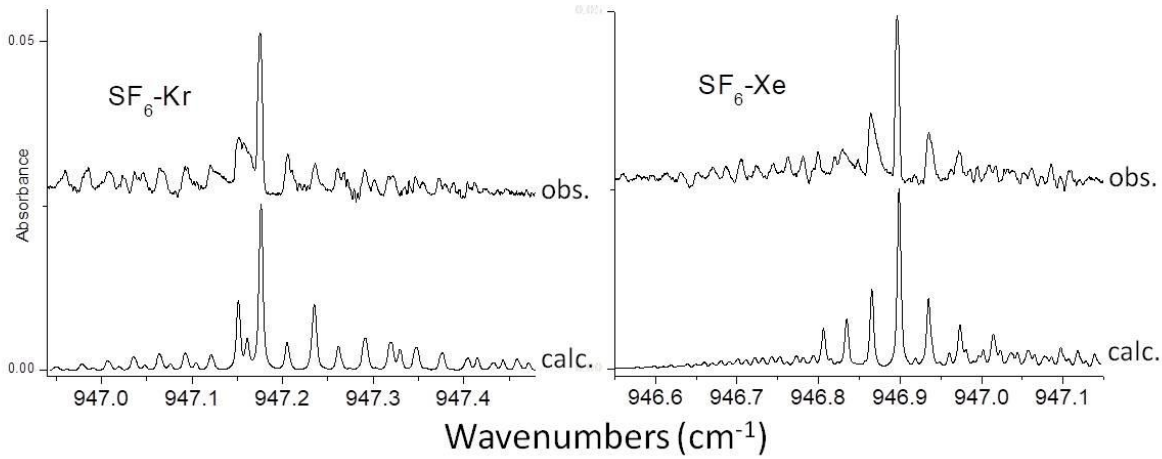

Fig. 3: EC-QCL jet cooled pin hole spectra of both ν_3 perpendicular bands of SF_6-Rg heterodimers (Rg= Kr, Xe) with 0.12 % SF_6 and 1% Rg diluted in 8 bar helium at an axial distance z = 15 mm, compared to our best simulation. The rotational temperature used for these simulations is 0.7(1) K.

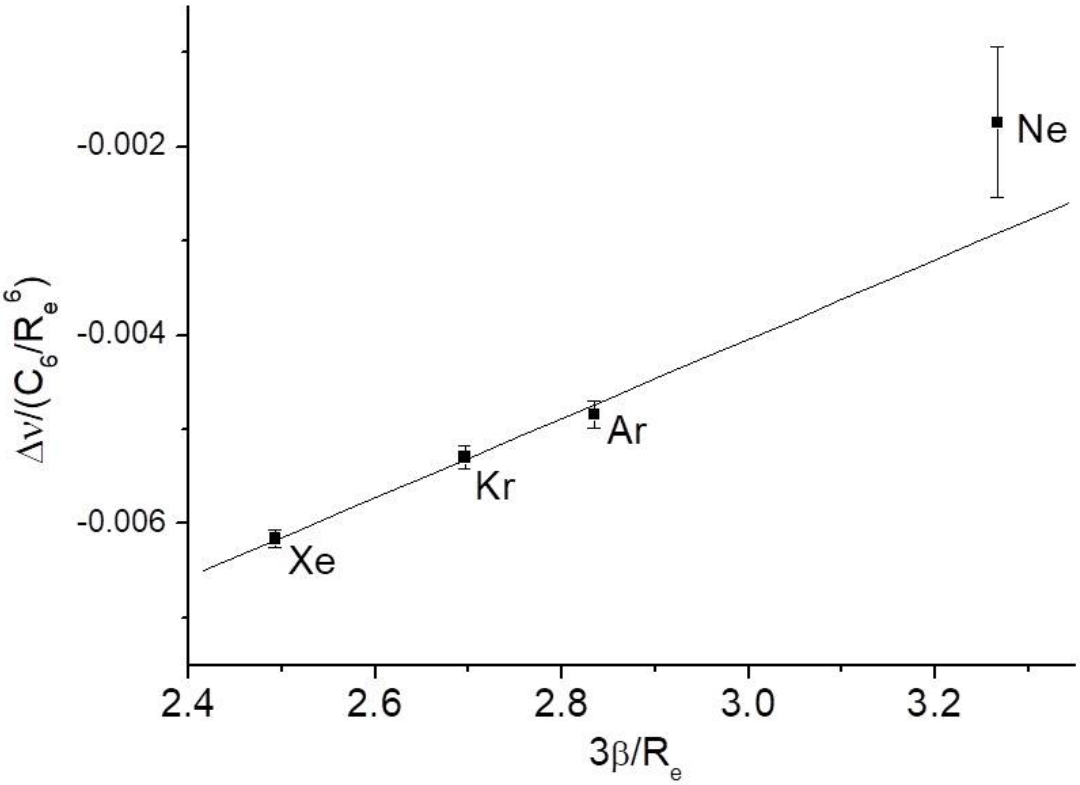

Fig. 4: Plot of the $\Delta\nu_{exp}$ (R_e^6/C_6) and $(3\beta/R_e)$ terms for the complexes SF_6-Rg and linear correlation obtained, in agreement with the predictions based on a Buckingham-type intermolecular potential (see text and Eq. 7).

	SF_6-Xe	SF_6-Kr	SF_6-Ar
	Parallel band		
A''/cm^{-1}	0.0874[(a)]	0.0874[(a)]	0.0874[(a)]
B''/cm^{-1}	0.010382(6)	0.014158(17)	0.022765(45)
A'/cm^{-1}	0.087261(35)	0.086956(59)	0.086804(85)
B'/cm^{-1}	0.010102(6)	0.013535(14)	0.020733(36)
ν_0/cm^{-1}	946.22327(18)	946.64108(30)	946.97950(48)
$R_0(SF_6 - Rg)$/pm	456.17(13)	434.60(26)	420.82(42)
$R_e(SF_6 - Rg)$/pm[(d)]	459.25(13)	439.38(28)	430.21(44)
	Perpendicular band		
A''/cm^{-1}	0.0874[(a)]	0.0874[(a)]	0.0874[(a)]
B''/cm^{-1}	0.010382[(b)]	0.014158[(b)]	0.022765[(b)]
A' /cm^{-1}	0.08865(17)	0.10471(14)	-
B'/cm^{-1}	0.010395(7)	0.014296(13)	-
ν_0/cm^{-1}	946.94171(37)	947.22478(39)	947.392[(c)]
ξ	0.687(2)	0.663(2)	

[(a)] RI-DFT-D *ab initio* value of A".
[(b)] Ground state B" constants for the perpendicular band analyses are fixed to the B" values derived from the parallel band analyses.
[(c)] The ν_0 frequency for the perpendicular band of SF_6-Ar corresponds to the maximum of the $^{R}Q(J,0)$ branch.
[(d)] The equilibrium B_e ground state necessary to determine R_e is derived from the relation B_e= B'' + $\alpha/2$ where α = B''-B' represents the vibration-rotation interaction constant.

Table 1: Molecular parameters (rotational constants, band centers and S-Rg distances) for the ground and ν_3 parallel and perpendicular states of the van der Waals SF_6-Rg heterodimers (Rg= Ar, Kr, Xe) derived from the band contour analyses of EC-QCL jet-cooled pin hole spectra.

	SF_6-Rg				SF_6-Rg_2				SF_6-Rg_3	
	$\Delta\nu_{\perp}$	$\Delta\nu_{//}$	$\boldsymbol{\Delta\nu_{exp}}$	$\Delta\nu_{th}$	$\Delta\nu_1$	$\Delta\nu_2$	$\Delta\nu_3$	$\boldsymbol{\Delta\nu_{exp}}$	$\Delta\nu_1$	$\Delta\nu_2$
red shifts (cm^{-1})										
Ne			0.12[(a)]							
Ar	0.585	1.000	**0.723**	*0.448*	1.284	1.494	1.755	***1.511***	-	2.313
Kr	0.802	1.339	**0.981**	*0.570*	1.736	2.045	2.365	***2.049***	2.657	-
Xe	1.08	1.756	**1.305**	*0.694*	2.120	2.607		**-**		
relative red shifts										
Ar	0.809	1.383	**1**		1.776	2.067	2.427	***2.090***	--	3.199
Kr	0.818	1.365	**1**		1.770	2.085	2.411	***2.088***	2.708	
Xe	0.828	1.346	**1**		1.625	1.998	--			

[(a)]*Estimate of the Q branch maximum from the subtraction spectrum of SF_6-Ne (see Fig. 1)*

Table 2: Experimental ν_3 red shifts (*upper panel*) observed for the parallel and perpendicular bands of the SF_6-Rg heterodimer and the three bands of the SF_6-Rg_n heteroclusters in the series of EC-QCL jet-cooled pinhole spectra. For each rare gas, the experimental shifts $\Delta\nu_{exp}$ (calculated according to relation (1)), are compared to the theoretical shifts ($\Delta\nu_{th}$ in italics) derived from a pure induction model[42] ; *lower panel*: relative red shifts after normalization by the experimental red shift ($\boldsymbol{\Delta\nu_{exp}}$ in bold), of the 1:1 complex, showing that the spectra of the several rare gases obey very similar patterns.

	Experimental R_e(S-Rg) distance	Calc. (RI-DFT-D) Minimum	C_{3v} constrained	*Relative difference (%) Calc. vs. Exp.*	Combination rules (CR)	*Relative difference (%) CR vs. Exp*
Ne-Ne	309.1[(a)]					
Ar-Ar	375.7[(a)]	401	-	*+ 6.7*		
Kr-Kr	401.1[(a)]	413.5	-	*+ 3.1*		
Xe-Xe	436.6[(a)]	456.6	-	*+ 4.6*		
SF_6-Ne		426.0	420.9		390	-
SF_6-Ar	430.2 [(b)]	441.7	440.3	*+ 2.3*	423	*- 1.7*
SF_6-Kr	439.4 [(b)]	455.7	451.4	*+ 2.7*	436	*-0.8*
SF_6-Xe	459.2 [(b)]	475.8	471.6	*+ 2.7*	454	*- 1.1*

[(a)] Interatomic distances (in pm) of rare gas dimers derived from the interatomic potential built by fitting empirically experimental data (Aziz et al.)[35-38]
[(b)] Present data; see Table 1 for precision

Table 3: Comparison between experimental $R_e(SF_6–Rg)$ distances obtained from the present high resolution infrared jet-cooled study and theoretical SF_6-Rg distances calculated from RI-DFT-D *ab initio* method (B97D3/def2-TZVPPD) and from combination rules for intermolecular distances.

	Ɛ (cm^{-1})			D_0(cm^{-1}) (Ɛ -ZPE)
	combination rules	Buckingham potential	DFT-D quantum chemistry	quantum chemistry
SF_6-Ne	97	104	92	48
SF_6-Ar	178	227	197	145
SF_6-Kr	211	283	244	197
SF_6-Xe	250	322	303	267

Table 4 : Well depths Ɛ of the SF_6-Rg dimers : Comparison between quantum chemistry calculations (BSSE-corrected B97-D3/def2-TZVPPD level of theory), estimations from combination rules (obtained from the geometrical mean of the homodimer wells) and from the Buckingham potential (Formula (4) with parameters reported in Tables S2 and S3 of Supp. Material). The last column displays the dissociation energies D_0 obtained by quantum chemistry at the same level of theory.

References

[1]M. Rossi, W. Fang and A. Michaelides, J. Phys. Chem. Lett. 2015, **6**, 4233.
[2]J. S. Muenter, *in* ''Atomic and Molecular Beam Methods'' (G. Scoles, Ed.), Vol. 2. Oxford University Press, Oxford, 1995.
[3] A. C. Legon, *in* ''Atomic and Molecular Beam Methods'' (G. Scoles, Ed.), Vol. 2. Oxford University Press, Oxford, 1995.
[4] D.W.Pratt, Annu. Rev. Phys. Chem. 1998, **49**, 481.
[5] H.J. Neusser, R. Sussman, in *Jet Spectroscopy and Molecular Dynamics*, eds. J.M. Hollas, D. Phillips, Springer Media, New York 1995, 118.
[6] B.J. Howard and A.S. Pine, Chern. Phys. Lett. 1985, **122**, 1.
[7] G. T. Fraser and A. S. Pine, J. Chem. Phys. 1986, **85**, 2502.
[8] D. T. Anderson, S. Davis and D. J. Nesbitt, J. Chem. Phys. 1997, **107**, 1115.
[9] Z. S. Huang, K. W. Jucks and R. E. Miller , J. Chem. Phys. 1986, **85**, 6905.
[10] R. W. Randall, M. A. Walsh, and B. J. Howard, Faraday Discuss. Chem. Soc. 1988, **85**, 13.
[11] G. T. Fraser, A. S. Pine, and R. D. Suenram, J. Chem. Phys. 1988, **88**, 6157.
[12] M. Iida, Y. Ohshima, and Y. Endo, J. Chem. Phys. 1993, **97**, 357.
[13] T. A. Hu, E. L. Chappell, and S. W. Sharpe, J. Chem. Phys. 1993, **89**, 6162.
[14] W. A. Herrebout, H-B Qian, H. Yamaguchi and B. J. Howard, J. Mol. Spectrosc. 1998, **189**, 235.
[15] G. D. Hayman, J. Hodge, B. J. Howard, J. S. Muenter, and T. R. Dyke, J. Chem. Phys. 1987, **86**, 1670.
[16] Y. Xu and M. C. L. Gerry, J. Mol. Spectrosc. 1995, **169**, 181.
[17] Z. Abusara, L. Bovayeh, N. Moazzen-Ahmadi, A. R. W. Mc Kellar, 2006, **125**, 144306.
[18] See https://wesfiles.wesleyan.edu/home/snovick/SN_webpage/vdw.pdf.
[19] R. Lascola and D. J. Nesbitt, J. Chem. Phys. 1995, **95**, 7917.
[20] X. Liu and Y. Xu, J. Mol. Spectrosc. 2014, **301**, 1.
[21] G. T. Fraser, A. S. Pine and W. A. Kreiner, J. Chem. Phys. 1991, **94**, 7061.
[22] P. Asselin, Y. Belkhodja, A. Jabri, A. Potapov, J. Loreau and A. van der Avoird, Mol. Phys. DOI: 10.1080/00268976.2018.1471533 (2018).
[23] G. M. Hansford and P. B. Davies, J. Chem. Phys. 1996, **104**, 8292.
[24] T. E. Gough, D.G. Knight and G. Scoles, Chem. Phys. Lett. 1983, **97**, 155.
[25] X.J. Gu, D. J. Levandier, B. Zhang, G. Scoles and D. Zhuang, J. Chem. Phys. 1990, **93**, 4898.
[26] R-D. Urban, L. G. Jörissen, Y. Matsumoto and M. Takami, J. Chem. Phys. 1995, **103**, 3960.
[27] M. Hartmann, R. E. Miller, J. P. Toennies and A. F. Vilesov, Science, 1996, **272**, 1631.
[28] P. Asselin, A. Potapov, A. C. Turner, V. Boudon, L. Bruel, M-A. Gaveau, M. Mons, Phys. Chem. Chem. Phys. 2017, **19**, 17224.
[29] P. Asselin, Y. Berger, T. R. Huet, R. Motiyenko, L. Margulès, R. J. Hendricks, M. R. Tarbutt, S. Tokunaga, B. Darquié, Phys. Chem. Chem. Phys. 2017, **19**, 4576.
[30] M. D. Brookes, C. Xia, J. A. Anstey, B. G. Fulsom, K.-X. Au Yong, J. M. King and A. R. W. McKellar, Spectrochim. Acta, Part A, 2004, **60**, 3235.
[31] D. R. Miller, in Atomic and Molecular Beam Methods, ed.G. Scoles, Oxford University Press, New-York, 1988, vol. 1.
[32] Ch. J. Bordé, M. Ouhayoun, A. van Lerberghe, C. Salomon, S. Avrillier, C. D. Cantrell, and J. Bordé, Laser Spectroscopy 4, edited by H. Walther and K. W. Rothe ~Springer, New York, 1979.
[33] S. Grimme, J. Comput. Chem. 2006, **27**, 1787.
[34] TURBOMOLE V6.4 2012, a development of University of Karlsruhe and Forschungszentrum Karlsruhe GmbH, 1989–2007, TURBOMOLE GmbH, since 2007; available from http://www.turbomole.com.
[35] R. A. Aziz and M. J. Slaman, Chem. Phys. 1989, **130**, 187.
[36] R. A. Aziz, J. Chem. Phys. 1993, **99**, 4518.
[37] A. K. Dham, A. R. Allnatt, W. J. Meath, and R. A. Aziz, Mol. Phys. 1991, **67**,1291.
[38] A. K. Dham, W. J. Meath, A. R. Allnatt, R. A. Aziz, and M. J. Slaman, Chem. Phys. 1990, **142**, 173.

[39] H. A Lorentz, Ann. Physik 1881, **12**, 127.
[40] R,J. Good and C.J. Hope, J. Chem.. Phys. 1971, **55**, 111.
[41] R. A. Aziz, M. J. Slaman, W. L. Taylor et J. J. Hurly, J. Chem. Phys. 1991, **94**, 1034.
[42] D. Eichenauer and R. J . Le Roy, J. Chem. Phys. 1988, **88**, 2898.
[43] T. A. Beu, Y. Okada and K. Takeuchi, Eur. Phys. J. D. 1999, **6**, 99.
[44] A. J. Stone, ‘‘The Theory of Intermolecular Forces,’’ Clarendon Press, Oxford, 1996.
[45] K. T. Tang and J. P. Toennies, J. Chem. Phys 2003, **118**, 4976.